Northumbria Research Link

Northumbria
University
NEWCASTLE

COMMUNICATION

Screen printing directed synthesis of covalent organic framework membranes with water sieving property

Received 00th January 20xx,
Accepted 00th January 20xx

DOI: 10.1039/x0xx00000x

Jialu Li,[a,b] Huazhen Rong,[b] Yifan Chen,[a] Hao Zhang,[b] Terence Xiaoteng Liu,[c] Ye Yuan,[b] Xiaoqin Zou*[b] and Guangshan Zhu[b]

Screen printing is introduced to direct the synthesis of crack-free and thickness-tunable $TpPa(OH)_2$ covalent organic framework membranes. A smooth precursor layer is firstly screen printed and then fully crystallised into $TpPa(OH)_2$ membrane. Molecular-scale pores endow the membrane fast water-sieving property, which is promising in water desalination.

Covalent organic frameworks (COFs), constructed from organic monomers through strong covalent bonds, are emerging as a new class of ordered porous materials with diversified structures, well-defined pores and high surface areas.[1-5] These properties together with polymer nature make COFs of great potential in various applications, in particular molecular separation.[6-9] COF membranes are considered more promising than COF bulk powders for gas or liquid separations owing to the integrated advantages of uniform pores and molecular affinity in COFs, easy operation and low energy consumption during membrane process. In this regard, many researchers commence the synthesis of COF membranes,[10-11] however, fabricating membranes with separation property is very challenging while it has been evidenced by only several limited successes in the last 5 years. One of the biggest hurdles in this research field is the lack of effective synthesis methods.

The methods reported up to date can be mainly categorised in the following: (1) solvothermal synthesis.[12-13] The COF membrane is grown directly on a solid support in solution under solvothermal condition. This method produced membranes are highly crystalline, however, the substrate dependence causes both difficulties on scale-up synthesis and membrane transfer from one substrate to another, which limits its wide application. (2) Interfacial polymerisation.[14-20] The monomers in two immiscible solvents counter diffuse to liquid-liquid or liquid-air interfaces and COF membranes are formed at these interfaces. This method can produce thin and free-standing membranes, but produced membranes are usually devoid of high compactness which leads to low separation performance. (3) Layer-by-layer stacking. This method generally consists of two steps: first exfoliation of bulk COFs into monolayers and then restack of the layers into COF membranes on supports.[21-23] In spite of the success in making separative membranes, this indirect method suffers from tedious exfoliation process and low yield of layered COFs. (4) Solid-state synthesis.[24-28] The monomers and catalyst are mixed into one batch and sintered straight on a support to form a COF membrane. Although membranes are conveniently produced through this method, uneven particles in the precursor cause the membrane continuity unsatisfactory in separation application, leaving a gap for membrane quality improvement.

To overcome the above limitations, herein, we propose an alternative and efficient approach - screen printing directed synthesis - to fabricate COF membranes, and the details are shown in Fig. 1a. A gel-like precursor containing 1,3,5-triformylphloroglucinol (Tp), 2,5-diaminohydroquinone dihydrochloride ($Pa(OH)_2$), p-toluene sulphonic acid (PTSA) and a small amount of water is prepared, and then placed atop the screen. A squeegee is pushed across the screen to transfer the precursor through the mesh openings onto a substrate. One thin film of precursor is printed at a time on the top of the substrate. Subsequently, the precursor film is heated and the crystallisation takes place to allow the formation of crystalline $TpPa(OH)_2$ COF membrane. This screen-printing process can produce uniform and thin precursor films by adjusting screen mesh and print cycle, which is prerequisite for the precise control on homogeneity and thickness of the COF membrane. This technique also offers facile synthesis of continuous COF membranes with different sizes, various shapes and high strength.

[a] *Department of Chemistry, Jilin University, 2699 Qianjin Street, Changchun 130012, China.*
[b] *Faculty of Chemistry, Northeast Normal University, 5268 Renmin Street, Changchun 130024, China.*
E-mail: zouxq100@nenu.edu.cn
[c] *Department of Mechanical and Construction Engineering, Faculty of Engineering and Environment, Northumbria University, Newcastle upon Tyne, NE1 8ST, UK.*
Electronic Supplementary Information (ESI) available: Experiments and supporting figures. See DOI: 10.1039/x0xx00000x

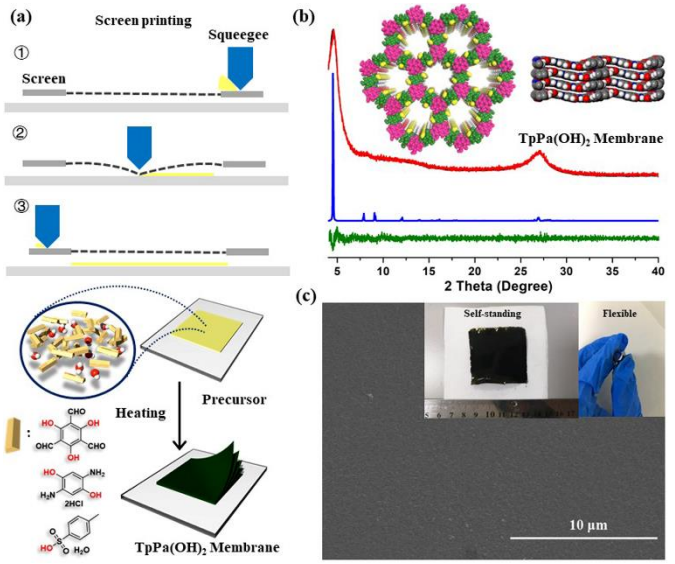

Fig. 1 (a) A schematic illustration of the screen printing synthesis for the $TpPa(OH)_2$ membrane, (b) XRD pattern and (c) top SEM image of the synthesised membrane (insets in (c) are digital photos of the membrane).

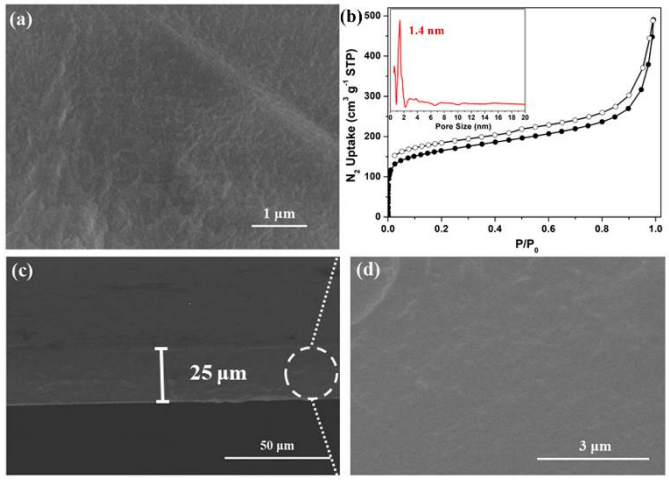

Fig. 2 (a) Top and (c) cross-section SEM images of the $TpPa(OH)_2$ membrane, (d) is an enlarged view of (c), and (b) the N_2 adsorption-desorption isotherm at 77 K of the $TpPa(OH)_2$ membrane (inset is its pore size distribution).

The appearance of –C–N band (1251 cm^{-1}) in the infrared spectrum (IR) of the $TpPa(OH)_2$ membrane confirms that the reaction between Tp and $Pa(OH)_2$ monomers occurs after stepwise heating from 50 °C to 120 °C (Fig. S1).[29-30] The synthesised membrane structure was characterised by powder X-ray diffraction (XRD) and the pattern is shown in Fig. 1b. Two diffractions associated with (100) and (001) planes are distinguished at 4.5° and 27°, in accordance with the simulated ones (Fig. S2), indicating that the $TpPa(OH)_2$ membrane adopts AA eclipsed stacking mode to form a 2D layered structure. Fig. 1c shows the morphology of the obtained $TpPa(OH)_2$ membrane. Optical pictures (insets in Fig. 1c) show that the membranes are self-standing and flexible, and the uniform colour indicates that the membrane is homogeneous with COFs. This is confirmed by the uniform distributions of C, N and O elements by scanning electron microscopy (SEM) mapping images of the membrane (Fig. S3). From top SEM images in Fig. 1c and Fig. 2a, the $TpPa(OH)_2$ membrane has no obvious cracks or pinholes under micron-scale magnification, revealing its high continuity. The membrane thickness is approximately 25 μm measured from the cross-section SEM image (Fig. 2c). The side view in Fig. 2d shows that the membrane is highly uniform, confirming that it is free of microscopic defects. To be noted, the membrane is very smooth evidenced both by the small relative standard deviation (1.47%) in the thickness (Fig. S4d) and the small roughness of the top membrane surface (Rq: 8.53 nm, Ra: 6.84 nm) in the atomic force microscopy (AFM) image (Fig. S5). The screen-printing synthesis approach is more advantageous to classical techniques such as knife casting[25] and glass casting[27] in fabricating smooth and uniform COF membranes (Fig. S6). The membrane uniformity probably stems from narrow size distribution of particles which are sieved by screen meshes in the gel precursor. Furthermore, the membrane thickness can be facilely tuned from 25 μm to 120 μm by repetitive printing of 1 to 5 times (once, thrice and quantic) (Fig. S4).

Fig. S7 shows the photos of circle, square and triangle $TpPa(OH)_2$ membranes, demonstrating that this method provides a simple way to adjust the membrane shape. Additionally, scale up synthesis of membrane is possible, evidenced by the large surface area of resultant membrane (up to ~25 cm^2) (Fig. S8). The N_2 adsorption-desorption isotherm of the $TpPa(OH)_2$ membrane at 77 K is shown in Fig. 2b. Brunauer-Emmett-Teller (BET) surface area of this membrane is estimated to be 598 m^2 g^{-1} and the total pore volume is calculated to be 0.58 cm^3 g^{-1}. The dominant pore size of this membrane is 1.4 nm (inset in Fig. 2b), in good agreement with the one from structure simulation (1.5 nm, Fig. 1b). Above results demonstrate that screen printing brings great benefits in the controlled synthesis of continuous and crystalline COF membranes (uniform pores, surface smoothness, precise membrane size, shape, strength and thickness).

SEM and XRD were applied to investigate the formation process of the $TpPa(OH)_2$ membrane in detail (Fig. 3). After sieving with screen mesh, the gel precursor made from PTSA, $Pa(OH)_2$, Tp and water contains a large number of rod-like particles (1-5 μm in length and 0.5-2 μm in width) (Fig. 3a), possibly originated from the formation of PTSA-$Pa(OH)_2$ salts along H-bonding direction.[25] PTSA is used for catalysing the reaction and served as a H-bonding reagent to improve monomers interactions.[25] When the precursor was heated at 50 °C for 6 h in water vapour atmosphere, some particles start to dissolve and merge together (Fig. 3b), rendering the gel become more homogenous, which is evidenced by a smoother surface in comparison to that of rough starting precursor (Fig. S9). With temperature increase, the dissolved $Pa(OH)_2$ species can participate in Schiff base reaction to link Tp components, promoting the occurrence of gelation. The undissolved reactants mainly remain the particle-shape state. As the temperature was programmed to 90 °C, most rod-like particles disappear (Fig. 3c). During current stage, XRD peak starts to evolve at 4.5°, corresponding to the diffraction of (100) plane (Fig. S10). This observation indicates that $Pa(OH)_2$ and Tp are assembled horizontally into a

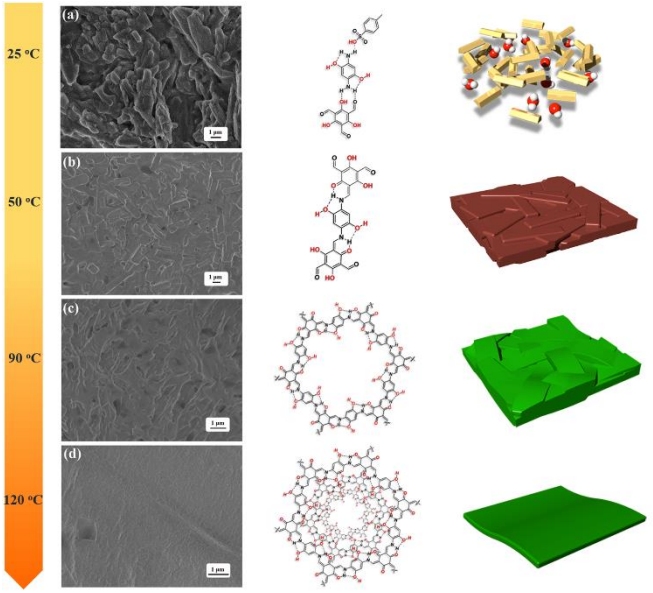

Fig. 3 Top-view SEM images of the $TpPa(OH)_2$ membrane in the growth process with a stepwise heating: (a) at 25 °C, (b) at 50 °C, (c) at 90 °C and (d) 120 °C, respectively; and the descriptions of possible molecular and membrane status for each corresponding stage in the growth process.

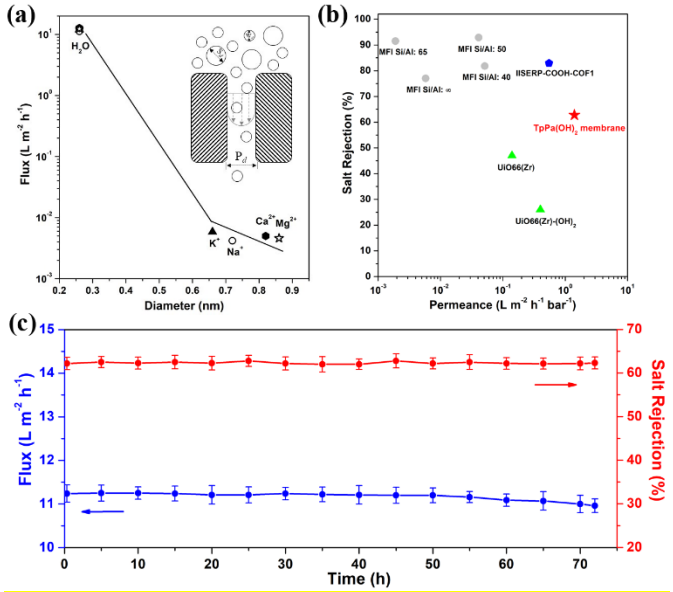

Fig. 4 (a) Water and cation fluxes of single salt solutions (salt concentration: 1000 ppm, feed pressure: 0.8 MPa) at 25 °C, (b) performances of $TpPa(OH)_2$ and other membranes applied in reverse osmosis water desalination, and (c) water flux and salt rejection in function of time for the $TpPa(OH)_2$ membrane (1000 ppm NaCl concentration, 25 °C operation temperature, 0.8 MPa feed pressure).

relatively regular structure *via* intensive crosslink of each other. After heat treated at 120 °C for 6 h, the crystallisation proceeds more completely which is shown by a peak with higher intensity at 4.5° (Fig. S10), and resulted in further growth along (100) direction of $TpPa(OH)_2$ crystals. As a consequence, a continuous membrane is formed (Fig. 3d).

To evaluate desalination property, the $TpPa(OH)_2$ membrane was subjected to sieve water from salts *via* reverse osmosis mode. Fig. 4a shows the fluxes of H_2O, Na^+, K^+, Mg^{2+} and Ca^{2+} in single-component aqueous solutions through this membrane. Water flux is almost three orders of magnitude higher than those of the cations. Rejection degrees of 62.9%, 51.4%, 60.7% and 62.8% are calculated respectively for Na^+, K^+, Ca^{2+} and Mg^{2+} cations according to cation concentration in feed and permeated solutions. This result can be ascribed to the fact that the small size of water and the hydrophilicity of hydroxyl groups in $TpPa(OH)_2$ favour the preferential transport of water molecules against solvated cations in the pores of the $TpPa(OH)_2$ membrane. The effectiveness for rejecting the penetration of cations through the membrane validates a good compactness of the $TpPa(OH)_2$ membrane. The imperfect rejection (~60% *vs* 100%) can be rationalized by the pore-flow characteristics of water and cation diffusions when the pore size (1.4 nm) is still larger than the solvated cation (0.66-0.86 nm).[31] Further improvement for ion rejection degree will be our focus in the future work. After the survey of all polycrystalline microporous membranes (zeolites, metal organic frameworks, covalent organic frameworks) in the related application, it can be found in Fig. 4b,[32-36] that the $TpPa(OH)_2$ membrane exhibits the highest water permeance (1.4 L m^{-2} h^{-1} bar^{-1}) and good Na^+ rejection degree (62.9%). In addition, the $TpPa(OH)_2$ membrane is very robust shown by constant water flux (11.2±0.5 L m^{-2} h^{-1}) and rejection degree of sodium ion (62.9%±0.9%) during consecutive implementation for 72 h (Fig. 4c). The superior cation separation property along with the excellent stability makes this membrane promising in water desalination.

In summary, for the first time, we introduced the screen-printing directed synthesis approach to fabricate flexible and continuous $TpPa(OH)_2$ COF membranes. This approach showcased fine control on crystallinity, thickness, shape and size of the $TpPa(OH)_2$ membrane by simple adjustment of the precursor and crystallisation process. The synthesised membrane exhibited high water permeance owing to porous structure of $TpPa(OH)_2$ and appreciable ion exclusion for a variety of cations during reverse osmosis desalination due to hydrophilic pores with suitable size. This study not only provides a guideline for the fabrication of high-quality COF membranes, but also sheds a light of the potential application of COF membranes for water desalination.

Conflicts of interest

There are no conflicts to declare.

Acknowledgements

We are grateful to the financial supports from National Natural Science Foundation of China (NSFC grant no. 21531003, 21501024, 21971035), Jilin Scientific and Technological Development Program (20170101198JC, 20190103017JH), Jilin Education Office (JJKH20180015KJ), "111" Program (B18012), lab open projects from State Key Laboratory of Inorganic Synthesis and Preparative Chemistry (2018-8), State Key Laboratory of Heavy Oil Processing (SKLOP201902003), and

Engineering & Physical Sciences Research Council (EPSRC) (EP/S032886/1).

Notes and references

1 X. Feng, X. S. Ding and D. L. Jiang, *Chem. Soc. Rev.*, 2012, **41**, 6010-6022.
2 P. J. Waller, F. Gandara and O. M. Yaghi, *Acc. Chem. Res.*, 2015, **48**, 3053-3063.
3 A. P. Cote, A. I. Benin, N. W. Ockwig, M. O'Keeffe, A. J. Matzger and O. M. Yaghi, *Science*, 2005, **310**, 1166-1170.
4 S. Y. Ding and W. Wang, *Chem. Soc. Rev.*, 2013, **42**, 548-568.
5 N. Huang, P. Wang and D. L. Jiang, *Nat. Rev. Mater.*, 2016, **1**, 16068.
6 M. S. Lohse and T. Bein, *Adv. Funct. Mater.*, 2018, **28**, 1705553.
7 Z. F. Wang, S. N. Zhang, Y. Chen, Z. J. Zhang and S. Q. Ma, *Chem. Soc. Rev.*, 2020, **49**, 708-735.
8 X. Jiang, S. W. Li, Y. P. Bai and L. Shao, *J. Mater. Chem. A*, 2019, **7**, 10898-10904.
9 Y. Q. Zhang, X. Q. Cheng, X. Jiang, J. J. Urban, C. H. Lau, S. Q. Liu and L. Shao, *Mater. Today*, 2020, DOI: 10.1016/j.mattod.2020.02.002
10 S. S. Yuan, X. Li, J. Y. Zhu, G. Zhang, P. Van Puyvelde and B. Van der Bruggen, *Chem. Soc. Rev.*, 2019, **48**, 2665-2681.
11 H. Wang, Z. T. Zeng, P. Xu, L. S. Li, G. M. Zeng, R. Xiao, Z. Y. Tang, D. L. Huang, L. Tang, C. Lai, D. N. Jiang, Y. Liu, H. Yi, L. Qin, S. J. Ye, X. Y. Ren and W. W. Tang, *Chem. Soc. Rev.*, 2019, **48**, 488-516.
12 H. W. Fan, A. Mundstock, A. Feldhoff, A. Knebel, J. H. Gu, H. Meng and J. Caro, *J. Am. Chem. Soc.*, 2018, **140**, 10094-10098.
13 H. W. Fan, J. H. Gu, H. Meng, A. Knebel and J. Caro, *Angew. Chem. Int. Ed.*, 2018, **57**, 4083-4087.
14 Z. F. Wang, Q. Yu, Y. B. Huang, H. D. An, Y. Zhao, Y. F. Feng, X. Li, X. L. Shi, J. J. Liang, F. S. Pan, P. Cheng, Y. Chen, S. Q. Ma and Z. J. Zhang, *ACS Cent. Sci.*, 2019, **5**, 1352-1359.
15 X. X. Guo, T. H. Mao, Z. F. Wang, P. Cheng, Y. Chen, S. Q. Ma and Z. J. Zhang, *ACS Cent. Sci.*, 2020, DOI: 10.1021/acscentsci.0c00260
16 D. B. Shinde, L. Cao, A. D. D. Wonanke, X. Li, S. Kumar, X. W. Liu, M. N. Hedhill, A. H. Emwas, M. Addicoat, K. W. Huang and Z. P. Lai, *Chem. Sci.*, 2020, DOI: 10.1039/d0sc01679a
17 Y. Li, Q. Wu, X. Guo, M. Zhang, B. Chen, G. Wei, X. Li, X. Li, S. Li and L. Ma, *Nat. Commun.*, 2020, **11**, 599.
18 K. Dey, M. Pal, K. C. Rout, H. S. Kunjattu, A. Das, R. Mukherjee, U. K. Kharul and R. Banerjee, *J. Am. Chem. Soc.*, 2017, **139**, 13083-13091.
19 W. Y. Dai, F. Shao, J. Szczerbinski, R. McCaffrey, R. Zenobi, Y. H. Jin, A. D. Schluter and W. Zhang, *Angew. Chem. Int. Ed.*, 2016, **55**, 213-217.
20 M. Matsumoto, L. Valentino, G. M. Stiehl, H. B. Balch, A. R. Corcos, F. Wang, D. C. Ralph, B. J. Marinas and W. R. Dichtel, *Chem*, 2018, **4**, 308-317.
21 D. W. Burke, C. Sun, I. Castano, N. C. Flanders, A. M. Evans, E. Vitaku, D. C. McLeod, R. H. Lambeth, L. X. Chen, N. C. Gianneschi and W. R. Dichtel, *Angew. Chem. Int. Ed*, 2020, **59**, 5165-5171.
22 G. Li, K. Zhang and T. Tsuru, *ACS Appl. Mater. Inter.*, 2017, **9**, 8433-8436.
23 M. A. Khayum, S. Kandambeth, S. Mitra, S. B. Nair, A. Das, S. S. Nagane, R. Mukherjee and R. Banerjee, *Angew. Chem. Int. Ed.*, 2016, **55**, 15604-15608.
24 H. S. Sasmal, H. B. Aiyappa, S. N. Bhange, S. Karak, A. Halder, S. Kurungot and R. Banerjee, *Angew. Chem. Int. Ed.*, 2018, **57**, 10894-10898.
25 S. Kandambeth, B. P. Biswal, H. D. Chaudhari, K. C. Rout, H. S. Kunjattu, S. Mitra, S. Karak, A. Das, R. Mukherjee, U. K. Kharul and R. Banerjee, *Adv. Mater.*, 2017, **29**, 1603945.
26 A. Halder, M. Ghosh, M. A. Khayum, S. Bera, M. Addicoat, H. S. Sasmal, S. Karak, S. Kurungot and R. Banerjee, *J. Am. Chem. Soc.*, 2018, **140**, 10941-10945.
27 M. A. Khayum, V. Vijayakumar, S. Karak, S. Kandambeth, M. Bhadra, K. Suresh, N. Acharambath, S. Kurungot and R. Banerjee, *ACS Appl. Mater. Inter.*, 2018, **10**, 28139-28146.
28 K. Dey, H. S. Kunjattu, A. M. Chahande and R. Banerjee, *Angew. Chem. Int. Ed.*, 2020, **59**, 1161-1165.
29 S. Chandra, D. R. Chowdhury, M. Addicoat, T. Heine, A. Paul and R. Banerjee, *Chem. Mater.*, 2017, **29**, 2074-2080.
30 S. Wang, Q. Y. Wang, P. P. Shao, Y. Z. Han, X. Gao, L. Ma, S. Yuan, X. J. Ma, J. W. Zhou, X. Feng and B. Wang, *J. Am. Chem. Soc.*, 2017, **139**, 4258-4261.
31 J. R. Werber, C. O. Osuji and M. Elimelech, *Nat. Rev. Mater.*, 2016, **1**, 16018.
32 X. L. Liu, N. K. Demir, Z. T. Wu and K. Li, *J. Am. Chem. Soc.*, 2015, **137**, 6999-7002.
33 X. R. Wang, L. Z. Zhai, Y. X. Wang, R. T. Li, X. H. Gu, Y. D. Yuan, Y. H. Qian, Z. G. Hu and D. Zhao, *ACS Appl. Mater. Inter.*, 2017, **9**, 37848-37855.
34 L. X. Li, N. Liu, B. McPherson and R. Lee, *Ind. Eng. Chem. Res.*, 2007, **46**, 1584-1589.
35 L. X. Li, J. H. Dong, T. M. Nenoff and R. Lee, *J. Membr. Sci.*, 2004, **243**, 401-404.
36 C. Y. Liu, Y. Z. Jiang, A. Nalaparaju, J. W. Jiang and A. S. Huang, *J. Mater. Chem. A*, 2019, **7**, 24205-24210.

TOC:
An effective approach of screen printing has been developed to direct the synthesis of continuous COF membranes. The prepared membranes exhibit fast and selective water permeation property.